Heliyon 6 (2020) e04065

Contents lists available at ScienceDirect

Heliyon

journal homepage: www.cell.com/heliyon

Review article

Design and capital cost optimisation of three-phase gravity separators

Tariq Ahmed [a,*], Paul A. Russell [b], Nura Makwashi [a], Faik Hamad [b], Samantha Gooneratne [b]

[a] Department of Chemical and Petroleum Engineering, Bayero University Kano, Nigeria
[b] School of Computing, Engineering and Digital Technologies, Teesside University, UK

ARTICLE INFO

Keywords:
Chemical engineering
Petroleum engineering
Organic chemistry
Mathematical modeling
Petroleum industry
Three phase separator
Oil and gas
Capital cost
Mathematical optimisation

ABSTRACT

The separation of produced fluids is essential once it reaches the surface. This separation is achieved in gravity separators. The design and sizing of separators can be challenging due to the number of factors involved. Improper separator design can bottleneck and reduce the production of the entire facility. This paper describes the development of a capital cost optimisation model for sizing three phase separators. The developed model uses GRG Non-linear algorithms to determine the minimum cost associated with the construction of horizontal separators subject to four sets of constraints. A numerical sizing example was solved to provide the details associated with the model and the ease with which parameters can be varied to suit the user's needs. Finally, a spreadsheet comparison between results obtained from the developed model and four other extant models is carried out. Results indicated that the developed model predicted results within an absolute error of $\pm 5m^3$ in most cases and a maximum of $\pm 12.5m^3$ for very high gas flows in comparison to conventional models developed based on retention time theory.

1. Introduction

Over the years the composition of produced fluids has changed [1]. This can be attributed to increasing demand and reducing supply of easily produced oil which has led to the introduction of enhanced oil recovery techniques and production from deeper wells. Hence, the types of reservoirs now in production, use of enhanced oil recovery techniques and the increasing concern about damage to the environment, dictate that the design and operation of the surface separation techniques used to recover the oil from the produced fluids are re-examined and adapted for the current market demands. Three-Phase Separators are the key component surface separation equipment [2].

It has been established that some of the main factors affecting gas, oil, and water separation include; droplet size [3], physical properties of the fluids [4], and slenderness ratio [5]. A well-designed separator should separate the gas, oil, and water streams to ensure feeds to other downstream equipment are within design specifications. These include, a clean gas stream to prevent compressor breakdown, a pure oil stream to avoid pump cavitation, pipeline corrosion and hydrate formation, and finally a pure water stream to minimise hydrocarbon loss as well as minimise produced water treatment cost. To achieve these functions, several conventional separator sizing models have been developed based on retention time and droplet settling theory. In some cases, the droplet settling is used for the separation of liquid from the gravity settling section while the retention time theory is used for liquid-liquid separation [4], [6,7,8].

The limitation of the conventional sizing models is that they require a great deal of experience, involve extensive table lookups, and uses empirical constants. Therefore, more sophisticated design models have been developed using computational fluid dynamics and computational algorithms. CFD models [9, 10, 11, 12] are used to model the dynamics and hydrodynamics of phases and flows in three-phase separators. They are mostly used to determine the effect of the separator internals from which modifications can be made to improve the performance of the separator [13, 14, 15]. Computational algorithm models [16, 17]involve mathematical programming techniques that are flexible and can be assessed to determine the optimality of generated designs. These models unlike CFD models are used to determine the dimensions of the separator. A limitation of these models is that they are over-constrained and often limit the separator design to empirical constants set by conventional separators such as a slenderness ratio of 3–5.

This work presents the development of a capital cost optimisation model that aims to link the design of the separator to the economic costs associated with its construction. The model is based on capital cost minimisation using Generalised Reduced Gradient (GRG) Non-linear algorithms in excel. The model provides accurate separator dimensions

* Corresponding author.
E-mail address: T.Ahmed@tees.ac.uk (T. Ahmed).

https://doi.org/10.1016/j.heliyon.2020.e04065
Received 23 August 2019; Received in revised form 30 March 2020; Accepted 21 May 2020

with transparent calculations that do not rely on arbitrary table look-ups for constants that are not clearly defined.

2. Economic analysis

The first task in preparing an economic evaluation of a process deals with obtaining a capital cost estimate. Different cost estimating methods have different errors and accuracy [18]. Ideally, the cost estimate of a specific plant can be obtained by costing the individual plant equipment. The capital cost of a piece of chemical equipment is usually a function of its size, the type of material used for its fabrication, design temperature, and design pressure [19]. As such the simplest way to determine the capital cost of equipment is to multiply the equipment size by the cost per unit size provided by vendors. Cost per unit size can also be obtained from literature in the form of graphs and charts [20]. This process is referred to as cost estimation using correlations. Cost correlations do not start from the origin because even for very low capacities, there is some overhead costs associated with the equipment. Cost correlations have a slope of 1 meaning that the cost increases to infinity. At this point, it is more economical to install multiple units rather than one [21]. Eq. (1) also known as the "six-tenths rule" is obtained for intermediate capacity range. The "sixth-tenths rule" states that 'the ratio of cost of two plants producing the same product is proportional to the ratio of their capacities raised to the power of 0.6'.

$$C = C_B\left(Q/Q_B\right)^m \tag{1}$$

Where C_B and Q_B are the cost and capacity of a predetermined size, m is usually from 0.48 to 0.87 with an average value of 0.6. Often, the cost of equipment has to be converted to account for inflation. Cost indices are used in such cases using Eq. (2). The cost indices are published monthly or annually such as Chemical Engineering (CE) Plant Cost Index, etc.

$$C_2 = C_1\left(I_2/I_1\right) \tag{2}$$

Where I represent the relevant index and C_1 and C_2 represent different time periods.

A second method of estimating the capital cost is the factorial method. Similarly, this method is based on an estimate of the purchase cost of major equipment required for a process. However, other costs are estimated as factors of the equipment cost [22]. This method is attributed to Lang and has been used extensively to estimate the capital cost of process plants using Eq. (3).

$$C_F = C_u F_L \tag{3}$$

Where C_F is the fixed investment, C_U is the cost of major items of processing equipment and F_L are the factors for the direct cost. Lang proposed different values of F_L for different processing plant.

Over the years, the Lang factor method has been modified to improve its accuracy especially since only one factor is used [23]. Hand suggested the use of equipment type factors rather than plant type which implies more details. Guthrie [24] proposed a module-based technique which was later improved by Ulrich [25]. These methods consider the plant as a set of modules where each module consists of similar items. In module based techniques, the cost of each module is calculated, and material and pressure corrections are also applied. Irrespective of the cost estimate method applied, the overall objective of process plants is to a make profit. One way of achieving this objective is through mathematical optimisation, which involves the selection of the best element from a set of available elements.

3. Mathematical optimisation

Mathematical optimisation involves formulating an objective function that can be minimised or maximised to an optimal solution for a set of independent variables. This method has been used extensively in chemical and process design. To achieve this, the problem must be designed to fit into the following general form;

$$Optimize: y = f(X_1, X_2 \ldots, X_n) \tag{4}$$

$$Subject\ to:\ h_j(x_1, x_2, \ldots, x_n)\left\{\begin{matrix}\leq\\=\\\geq\end{matrix}\right\} b_j\ \ j = 1, 2, \ldots m \tag{5}$$

Where, Eq. (4) is the objective function, which is maximised or minimised subject to Eq. (5), which is the set of constraints imposed on the solution. The variables x_1, x_2, …, x_n are the set of decision variables. The constraints are expressed as equalities and inequalities. Satisfying all the constraints renders a feasible solution.

Different algorithms are available for solving Mathematical optimisation problems. Therefore, it is important to choose the right algorithms for each optimisation problem. In this case, due to the nonlinearity in both the objective function and the constraints, the Generalised Reduced Gradient (GRG) was chosen to optimize the separator design. This method has been proven to be effective and efficient for such problems [26]. The basic concept of GRG involves linearizing the non-linear objective and constraint functions at a local solution with the Taylor expansion Equation.

$$f(X) = f(X_1) + f'(X_1)(X - X_1) \tag{6}$$

$$h_i(x) = h_i(x_1) + h_i'(x_1)(x - x_1)\ i = 1,\ \ldots, m \tag{7}$$

The variables are divided into two subsets of basic (x) and non-basic (x) variables using the concept of reduced gradient. The basic variables are then expressed in terms of the non-basic variables using the concept of implicit variable elimination. The constraints are finally eliminated, and the variable space is reduced to non-basic variables only. Other proven methods for non-constrained non-linear optimisation problems are then employed to solve the approximated problem. The next optimal solution for the approximated problems is obtained in this manner and the process repeats until the optimal conditions are met [27].

3.1. Model theoretical design

An objective function and some constraints are required for mathematical optimisation. A generalised form of the optimisation problem is presented in Eqs. (9) and (10).

$$\text{Minimise: Cost (C)} = \text{function of (Capital cost)} \tag{9}$$

Subject to;

$$\begin{matrix}\text{Outlet Safety Constraints}\\ \text{Gravity Settling Section Constraint}\\ \text{Logical and Geometrical Constraints}\\ \text{Decision Variable Constraints}\end{matrix} \tag{10}$$

The optimisation problem consists of many adjustable variables that would be difficult to fix by traditional trial and error approaches. As such, the General Reduced Gradient (GRG) non-linear algorithms were chosen as the minimisation function for this model due to the non-linearity in the separator design and to counteract the excessive number of independent variables and constraints. The GRG solver uses an iterative numerical method that uses trial values for the adjustable cell and observes the

results calculated by the constraint cells and the optimum cell. The GRG solver performs an extensive analysis of the observed output and their rate of change as the inputs changes, to guide the selection of trial values. The flow diagram in Figure 1 explains how the model works.

Summary of Programme

- Start the spreadsheet model
- Input Initial guesses
  - Diameter (Di) $= D_{i1} = \left(\frac{4Q}{\pi U_v}\right)^{0.5}$
  - Normal operating level (NOL) = Di/2
  - Normal Interface Level (NIL) = Di/4
  - Length (VL) = Di x 4
- Calculate Mean Diameter (Dm)
- Calculate Length of gravity settling section
- Select the maximum length of gravity settling section.
- The maximum length selected is used to calculate the vessel length
- The vessel shell thickness is then calculated
- This is then used to calculate the vessel cost
- All the constraints are then calculated
- The GRG solver then uses an iterative numerical method that uses trial values for the adjustable cell and observes the results calculated by the constraint cells and the optimum cell.
- The GRG solver performs an extensive analysis of the observed output and their rate of change as the inputs changes, to guide the selection of trial values
- The dimensions (i.e. diameter and vessel length) that produced the minimum Vessel Cost and also satisfies all the constraints are chosen as the output.
- Once stopped the values for all the ten liquid levels inside the separator as well as the inlet and outlet dimensions, and weir height are obtained.

The first step involves the input of initial guesses for the length and diameter of the separator, normal operating level, and normal interface level. The inputted values are used to calculate the vessel mean diameter. The length requires for gravity settling is then calculated for; gas, oil and water. The maximum length for gravity settling is then selected from the three. This length is used to calculate the total vessel length. The vessel thickness and vessel cost (objective function) are calculated next. The constraints are then calculated. Once valid, the objective function is minimised, and the process is repeated until the minimum vessel cost is obtained that satisfies all the constraints. At this point an optimal solution is obtained and the separator dimensions and capital cost are obtained. The following sections provide more details on the model objective function and constraints and how each parameter is calculated.

3.1.1. *Objective function*

It was decided to base this model on an objective function formed from capital variables. Note that in this work, only the capital cost is considered. Once the vessel dimensions are obtained, it can be used to obtain the Separation Performance Indicator (SPI), and then the operating cost can be determined. The capital cost is based on the work carried out by Powers [8] for determining the capital cost of a horizontal vessel (see Equation 11).

$$C = fF_c\rho_s\left(\pi D_m^2 VL + 2F_aF_hD_m^3\right) \tag{11}$$

Where C is the vessel capital cost, f is the vessel thickness, F_C is the cost per unit mass to manufacture a vessel shell, ρ_s is density of steel, D_m is the vessel mean diameter, VL is the vessel length, F_a is the factor for determining surface area of a vessel head from vessel diameter squared, F_h is the ratio of cost per unit mass to manufacture a vessel head compared with that of vessel shell.

Eq. (11) can be broken down into input variables and calculated variables;

3.1.1.1. Input variables. These variables are divided into calculated input variable(s), manufacturer-supplied input variables, and constants. The vessel shell thickness is a calculated input variable. Vessel shell can be either thin or thick-walled. The rule of thumb used to differentiate between the two categories is that, for a thin-walled vessel, the vessel's diameter is an order of magnitude bigger than the vessel thickness, otherwise, it is categorised as a thick-walled vessel. Most separator

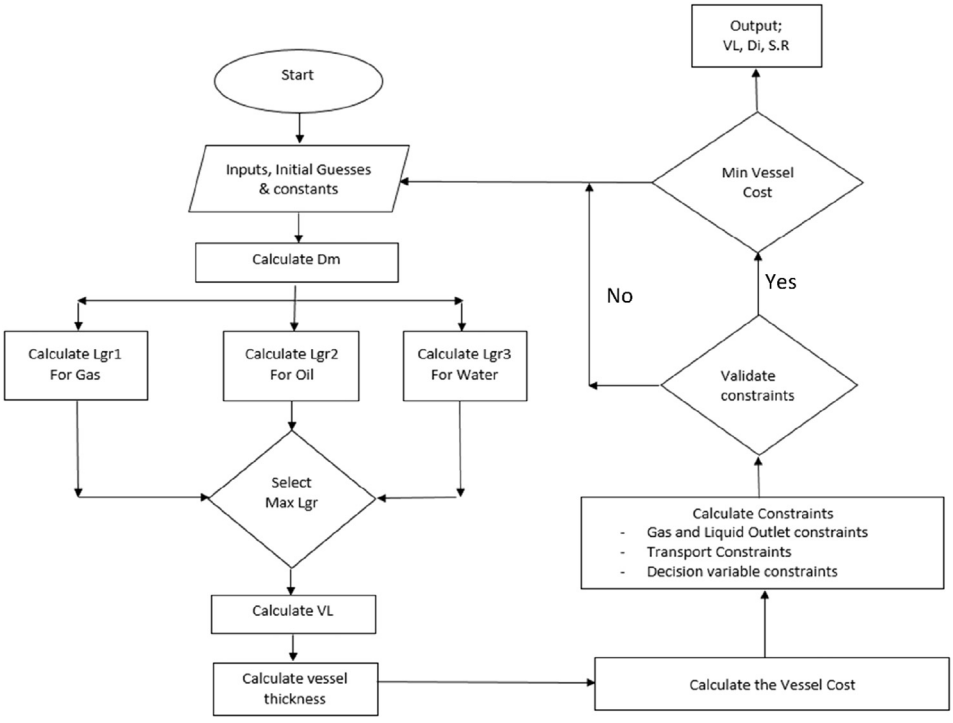

Figure 1. Process Flow Diagram for the current Model.

vessels in the process industries are thin-walled. The design, fabrication, and testing of pressure vessels is commonly based on the American Society of Mechanical Engineers (ASME) code for the design of pressure vessels [28]. This code is widely used in the oil and industry in the sizing of three-phase separators among other pressure vessels. Hence vessel shell thickness (thin-walled) is calculated using Eq. (12) [29].

$$f = \frac{P_D D_i}{2\sigma E - 1.2P_D} + t_c \tag{12}$$

The design pressure (P_D) (see Equation 13) is typically the maximum of either the operating pressure plus 10% or the operating pressure plus 15 to 30 psi [7]. Joint efficiency (E) ranges from 0.6 to 1, with 1 for a 100% x – rayed joint. The tensile strength (σ) of carbon steel commonly used due to its ability to withstand high temperature is 950bar. Corrosion allowance (tc) ranges from 1.6mm to 3.2mm

$$P_D = \max(1.1P,\ P + 200,000) \tag{13}$$

Manufacturer supplied input variables are supplied by the vessel manufacturer. They include the cost per unit mass to manufacture the vessel (F_c), factor for determining surface area of head from the vessel diameter (F_a) and the ratio of cost per unit mass to manufacture vessel head compared with the vessel shell (F_h). Default values of 5, 1.15 and 3 were included [11].

Finally, the last group of inputs in the objective function are the constants. These are pi (π) and the density of the carbon steel. Note that this value can be changed for other materials such as stainless steel.

3.1.1.2. Calculated variable. The vessel mean diameter and vessel length are the calculated variables. The vessel mean diameter (D_m) in Eq. (11) is obtained using Eq. (14).

$$D_m = \frac{D_i + (D_i + 2f)}{2} \tag{14}$$

Where Di is the separator internal diameter, f is the vessel shell thickness.

The separator internal diameter is fitted by the GRG function. However, it requires an initial guess (D_{i1}). Eq. (15) is used to obtain the initial guess for the model.

$$D_{i1} = \left(\frac{4Q}{\pi U_v}\right)^{0.5} \tag{15}$$

The vessel length also from Eq. (11) is calculated as the sum of the lengths of the separator inlet section, gravity settling section, and separator outlet section as shown in Eq. (16). The length of the separator inlet is usually the length required to mount the inlet device which should be at least twice the diameter of the separator inlet [30].

$$VL = L_i + L_{grv} + L_o \tag{16}$$

Similar to the separator internal diameter, the length of the gravity settling section is also fitted by the GRG function and therefore requires an initial guess. This is assumed to be four times the internal diameter (Di) calculated from Eq. (15). The length of the separator outlet section is calculated as the sum of twice the liquid outlets and the length of the weir as presented in Eq. (17). The oil and water outlets are calculated using Eq. (18) [7].

$$L_O = 2(d_{oo} + d_{no}) + L_{weir} \tag{17}$$

$$d_{po} = 0.146\sqrt{Q_p \times \rho_p^{0.5}} \tag{18}$$

Where d_{oo} and d_{wo} are the diameters of oi and water outlets, Lweir is the length of weir, d_{po} is the diameter of phase (oil or water) outlet, Q_p is the phase (oil or water) flow rate and ρ_p is the phase (oil or water) density.

Once the objective function is calculated, the next step is to determine the constraints. These are explained in the following section.

3.1.2. Constraints

The constraints that confine the objective function are divided into four groups.

3.1.2.1. Outlets safety constraints. A well-designed separator should produce outlet qualities specified for each product depending on the requirement and downstream process. If the normal operating level deviates far from its intended settings, the separator cannot produce acceptable effluents. Trip/shutdown levels were assigned at very low and very high levels (low-low interface level, high-high interface level, low-low liquid level, and high-high liquid level). This is to ensure the effluent quality is within the desired standard and to also protect downstream equipment such as pumps and compressors.

Alarm levels (low interface level, high interface level, low liquid level, and high liquid level) were assigned in between the shutdown levels to enable operators to intervene in cases where the automated control system is unable to manage the level [31]. Figure 2 present the separator with the ten liquid levels. The normal levels represent the oil levels while the interface levels represent the water level. The height between the liquid level and mist extractor inlet has been proposed by [14] and [16]. For this work, an average height of 0.175m is used as the safety factor between the liquid levels highlighted above.

The liquid levels presented in Figure 2 can be related to inlet oil and water flow rates through the Norsok Standard [32] and Holdup and Surge Equations. The Norsok standard states that "in the sizing of the separators, the equivalent residence time between normal and alarm level and between alarm and trip level should not be less than 30 s or 100mm whichever is greater, for both high and low ranges". This statement can be expressed as Eqs. (19) and (20) for normal levels and Eqs (21) and (23) for interface levels.

$$(Q_o + Q_w)\Delta t_{NS} \leq VL(A_a - A_b) \tag{19}$$

$$\Delta h_{Nor} \leq (h_a - h_b) \tag{20}$$

For interface levels, only the water flow rate is significant. Similarly, the length of the vessel available for interface control ends at the weir. Therefore, these two Equations can be represented as;

$$Q_w \Delta t_{NS} \leq Vl(A_x - A_y) \tag{21}$$

$$Vl = (L_I + L_{grv} + 2d_{wo}) \tag{22}$$

$$\Delta h_{Nor} \leq (h_x - h_y) \tag{23}$$

Where Q_o and Q_w are oil and water flow rate, Δt_{NS} is the time proposed by Norsok standard as 30 s, VL is the vessel length, Vl is the vessel length up to the weir, dwo is the water outlet diameter, Aa and Ab are the areas corresponding to liquid levels a and b. Li is the length of separator inlet section, L_{grv} is the length of gravity settling section, Δh_{Nor} is the height proposed by Norsok as 100mm, h_a and h_b are the height corresponding to liquid levels a and b. A_x and A_y are the areas corresponding to the interface levels x and y, h_x and h_y are the heights corresponding to interface levels x and y. Note that subscripts a and b are replaced by liquid levels whereas subscript x and y are replaced by interface levels as shown below.

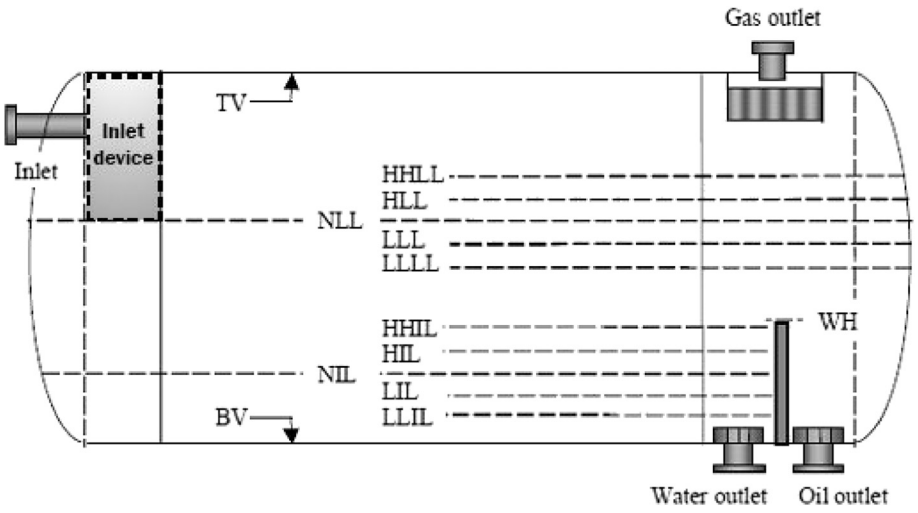

Figure 2. Separator Outlet Section showing outlet constraints. HHLL = High-high liquid level, HLL = High liquid level, NOL = Normal operating level, LLL = Low liquid level, LLLL = Low-low liquid level, HHIL = High-high interface level, HIL = High interface level, NIL = Normal interface level, LIL = Low interface level, LLIL = Low-low interface level, BV = Vessel bottom, TV = Vessel Top.

a = (LLL, NLL, HLL, HHLL) b = (LLLL, LLL, NLL, HLL)
x = (LIL, NIL, HIL, HHIL) y = (LLIL, LIL, NIL, HIL)

Holdup and surge volume Equations can be used to set a distance from the Normal operating level to the Low and High liquid levels using Eqs. (24) and (25).

$$V_{Holdup} = VL(A_{NOL} - A_{LLL}) \tag{24}$$

$$V_{surge} = VL(A_{HLL} - A_{NOL}) \tag{25}$$

For interface levels, the holdup and surge Equations are presented as Eqs (26) and (27);

$$V_{Holdup}\left(\frac{Q_w}{Q_o}\right) \leq Vl(A_{NIL} - A_{LIL}) \tag{26}$$

$$V_{Surge}\left(\frac{Q_w}{Q_o}\right) \leq Vl(A_{HIL} - A_{NIL}) \tag{27}$$

Where V_{Holdup} and V_{surge} are the holdup and surge volumes, A_{NOL} is the area of normal operating level, A_{LLL} is the area of low liquid level, A_{HLL} is the area of high liquid level, Q_w and Q_o are water and oil flow rates, Vl is the vessel length up to the weir, A_{NIL} is the area of normal interface level, A_{LIL} is the area of low interface level, A_{HIL} is the area of high interface level.

Note that the internal diameter of the separator (D_i), height of normal operating level (h_{NOL}) and height of normal interface levels (h_{NIL}) are initially inputted as guesses. The remaining liquid levels can then be calculated using the Equations above by substituting the subscripts a, b, x and y for the desired normal and interface levels respectively.

It is important to highlight that obtaining the separator levels using these Equations requires the conversion from height to area units and vice versa (see Figure 3). For simplicity, dimensionless parameters are used. Conventional separator sizing models use graph correlations to convert between these dimensionless quantities. In this work, Eqs. (28) and (29) are used to convert dimensionless chord Area ($A^* = A_H/A_T$) into dimensionless chord height ($H^* = h/D$). Note that this conversion requires an iterative approach and was therefore done as a function in the Excel spreadsheet. This process is referred to as ATOH in the subsequent Equations.

$$\varphi_{i+1} = \varphi_i - \frac{2\pi A^* - \varphi_i + \sin\varphi_i}{\cos\varphi_i - 1} \tag{28}$$

$$H^* = \frac{\left(1 - \cos\frac{\varphi}{2}\right)}{2} \tag{29}$$

Where φ_i is any initial guess, A is ratio of level area to total cross sectional area and H^* is the ratio of liquid height to the separator diameter.

Eqs. (30) and (31) are used together to calculate the dimensionless chord area from the dimensionless chord height. Similarly, this process is referred to as "HTOA" in the subsequent Equations.

$$\varphi = 2\cos^{-1}(1 - 2H^*) \tag{30}$$

$$A^* = \frac{(\varphi - \sin\varphi)}{2\pi} \tag{31}$$

As stated earlier in this section, for safe operation of the separator, a number of outlet constraints were put in place. These constraints are presented in the following subsections.

I. Avoid Oil from leaving through the Water outlet.

The first constraint was set to avoid oil from leaving through the water outlet. Therefore, the height of low-low interface level is set to be greater than or equal to 0.175m as shown in Eq. (32).

$$h_{LLIL} \geq 0.175m \tag{32}$$

The height of the low-low interface level can be calculated from the Area of low-low interface level using Eq. (33). Remember this requires conversion from area to height and hence the word "ATOH" which uses Eqs. (24) and (25).

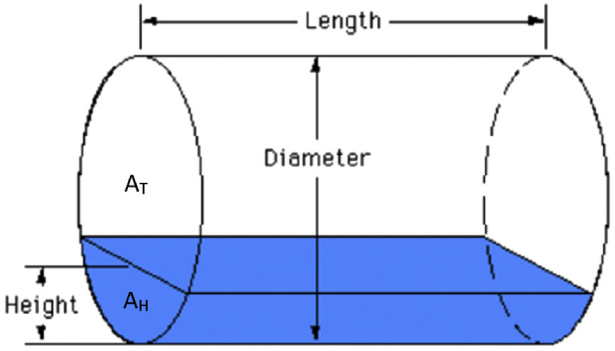

Figure 3. Cylinder partially filled with liquid.

$$h_{LLIL} = ATOH\left(\frac{A_{LLIL}}{A_T}\right) D_i \tag{33}$$

To calculate A_{LLIL} in Eq. (33), the minimum of Eqs. (21) and (23) is used. Substituting subscripts x and y for LIL and LLIL into 21 and 23 and making A_{LLIL} the subject of the formula gives Eqs. (34) and (35). Also note that Eq. (35) involves the conversion of height to area hence the use of "HTOA".

$$A_{LLIL} = A_{LIL} - \left(\frac{Q_w \Delta t_{NS}}{Vl}\right) \tag{34}$$

$$A_{LLIL} = HTOA\left(\frac{h_{LIL} - \Delta h_{NOR}}{D_i}\right) A_T \tag{35}$$

$$A_T = \frac{\pi D^2}{4} \tag{36}$$

In Eqs. (34) and (35) A_{LIL} is required. This is calculated by substituting x and y for NIL and LIL into Eqs. (21), (23), and (26) and solving for ALIL gives Eqs. (37), (38) and (39).

$$A_{LIL} = A_{NIL} - \left(\frac{Q_w \Delta t_{Nor}}{Vl}\right) \tag{37}$$

$$A_{LIL} = HTOA\left(\frac{h_{NIL} - \Delta h_{NOR}}{H_T}\right) A_T \tag{38}$$

$$A_{LIL} = A_{NIL} - \frac{V_{Holdup}\, Q_w}{Q_o Vl} \tag{39}$$

Height of Low interface level (h_{LIL}) in Eq. (35) is calculated from Eq. (40).

$$h_{LIL} = ATOH\left(\frac{A_{LIL}}{A_T}\right) D_i \tag{40}$$

The height of Normal interface level (h_{NIL}) in Eq. (37) is provided as an initial guess. A_{NIL} is obtained from h_{NIL} using Eq. (41)

$$A_{NIL} = HTOA\left(\frac{h_{NIL}}{D_i}\right) A_T \tag{41}$$

The height of low-low interface level and low interface level are obtained from the calculated area values. The next section presents the constraint and Equations for calculating the high interface level and high-high interface levels.

II. Avoid Water from leaving through the Oil outlet.

Three-phase separators are usually equipped with a weir for ease of interface level control. The weir is located in between the oil and water outlets and it is used to prevent the water phase from leaving through the oil outlet. To avoid overflow of the water into the oil section, the difference between the weir height and the high-high interface level is set to be equal to or greater than 0.175m as presented in Eq. (42). Failure to enforce this constraint in the separator might lead to water overflow into the oil compartment and leaving through the oil outlet.

$$h_{WH} - h_{HHIL} \geq 0.175m \tag{42}$$

The height of high-high inrerface level is calculated from the Area of high-high interface level.

$$h_{HHIL} = ATOH\left(\frac{A_{HHIL}}{A_T}\right) H_T \tag{43}$$

A_{HHIL} is obtained by substituting x and y for HHIL and HIL into Eqs. (21) and (23) which gives;

$$A_{HHIL} = \frac{Q_w{}^* \Delta t_{NS}}{Vl} + A_{HIL} \tag{44}$$

$$A_{HHIL} = HTOA\left(\frac{\Delta h_{NOR} + h_{HIL}}{D_i}\right) A_T \tag{45}$$

Substituting x and y for HIL and NIL into Eqs. (21), (23), and (27), and solving for A_{HIL} gives Eqs. (46), (47), and (48).

$$A_{HIL} = \frac{Q_w \Delta t_{NS}}{Vl} + A_{NIL} \tag{46}$$

$$A_{HIL} = HTOA\left(\frac{\Delta h_{NOR} + h_{NIL}}{D_i}\right) A_T \tag{47}$$

$$A_{HIL} = \frac{V_{Surge} Q_w}{Vl Q_o} + A_{NIL} \tag{48}$$

The maximum value obtained from Eqs. (46), (47), and (48) is used as the value for A_{HIL}. h_{HIL} is calculated from A_{NIL} using Eq. 49.

$$h_{HIL} = ATOH\left(\frac{A_{HIL}}{A_T}\right) H_T \tag{49}$$

h_{NIL} is assumed and used to calculate A_{NIL} using Eq. (50).

$$A_{NIL} = HTOA\left(\frac{h_{NIL}}{D_i}\right) A_T \tag{50}$$

The next section presents the constraint and Equations for calculating the height of the low-low liquid level and low liquid level.

III. Avoid gas from leaving through the liquid outlets.

The low-low liquid level was set to be the greather than the weir height as shown in Eq. (51). The weir height was set in the previous section to be a minimum of h_{HHIL} plus 0.175m. As such it has to be between the high high interface level and the low low liquid level. This constraint will prevent the gas phase from leaving through the oil outlet. Low-low liquid level height can be calculated from the area of the low-low liquid level. Note "HTOA" in the Equation converts height to area.

$$hLLLL \geq= h_{WH} + 0.175m \tag{51}$$

The area of low-low liquid level is calculated by substituting a and b for LLL and LLLL and solving for A_{LLLL} in Eqs. (19) and (20). Note "HTOA" in Eq (53) converts height to area.

$$A_{LLLL} = A_{LLL} - \left(\frac{(Q_O + Q_W)\Delta t_{NS}}{VL}\right) \tag{52}$$

$$A_{LLLL} = HTOA\left(\frac{h_{LLL} - \Delta h_{Nor}}{H_T}\right) A_T \tag{53}$$

Substituting 'a' and 'b' for NOL and LLL into Eqs. (19), (20), and (25), and solving for A_{LLL} gives Eqs. (54), (55), and (56).

$$A_{LLL} = A_{NLL} - \left(\frac{(Q_O + Q_W)\Delta t_{NS}}{VL}\right) \tag{54}$$

$$A_{LLL} = HTOA\left(\frac{h_{NOL} - \Delta h_{Nor}}{H_T}\right) A_T \tag{55}$$

$$A_{LLL} = A_{NLL} - \frac{V_{Holdup}}{VL} \tag{56}$$

A_{NOL} is calculated from Eq. (57).

$$A_{NOL} = HTOA\left(\frac{h_{NLL}}{H_T}\right) A_T \tag{57}$$

Calculate the h_{LLL} in Eq. (53) using Eq. (58).

$$h_{LLL} = ATOH\left(\frac{A_{LLL}}{A_T}\right) H_T \tag{58}$$

The height of low-low liquid level and low liquid level were calculated from the calculated area values. The next section presents the constraint and Equations for calculating high liquid level and high-high liquid levels.

IV. Avoid oil from leaving through the gas outlet.

The difference between the height of mist extractor inlet and the height of the high-high liquid level should be more than a safety factor as shown in Eq. (59).

$$h_{MEI} - h_{HHLL} \geq 0.175\text{m} \tag{59}$$

The Mist Extractor Inlet is obtained by subtracting the vessel diameter (Di) by 0.3m. Note that the difference between the internal diameter and high-high liquid level is set to be greater than 0.175m for separators without mist extractors. The mist extractor height is usually set to be 0.15m (6 inches). Another 0.15m is allowed from the top of the vessel to the mist extractor outlet. This height is set to obtain a uniform flow distribution through the extractor. If placed too close to the outlet nozzle, the extractor's efficiency will be reduced since most of the flow will be directed towards the centre. The height of high-high liquid level can be obtained from the area of High-high Liquid Level using Eq. (60).

$$h_{HHLL} = ATOH\left(\frac{A_{HHLL}}{VA}\right) D_i \tag{60}$$

Substituting 'a' and 'b' for HHLL and HLL into Eqs. (19) and (20) and solving for A_{HHLL} gives Eqs. (61) and (62).

$$A_{HHLL} = \left(\frac{(Q_o + Q_o)\Delta t_{Nor}}{VL}\right) + A_{HLL} \tag{61}$$

$$A_{HHLL} = HTOA\left(\frac{\Delta h_{Nor} + H_{HLL}}{H_T}\right) A_T \tag{62}$$

A_{HLL} can is calculated from the maximum of Eqs. (63), (64), and (65) obtained from Eqs. (19), (20), and (25).

$$A_{HLL} = \frac{(Q_o + Q_w)\Delta t_{Nor}}{VL} + A_{NLL} \tag{63}$$

$$A_{HLL} = HTOA\left(\frac{\Delta h_{Nor} + h_{NLL}}{D_i}\right) A_T \tag{64}$$

$$A_{HLL} = \frac{V_{surge}}{VL} + A_{NLL} \tag{65}$$

A_{NOL} is calculated using Eq. (57). The height of HLL is calculated from the Area of HLL using Eq. (66).

$$h_{HLL} = ATOH\left(\frac{A_{HLL}}{A_T}\right) D_i \tag{66}$$

All the liquid and interface levels are obtained using the outlet safety constraints presented in this section. The next section presents the gravity settling section constraints. These constraints were set to ensure the length of gravity settling is sufficient for the phases to separate.

3.1.2.2. Gravity setting section constraints. The minimum length required for gravity settling is set as a constraint. It can be calculated by setting the phase retention time in the vessel equal to the bubble/droplet rising/settling time (see Equation 68). For this model, rising/settling paths were assumed and used to calculate the lengths required for separation of the gas, oil, and water.

$$t_r \geq t_{og} \tag{68}$$

Three criteria that exist for this behaviour depending upon the bulk phase that is present:

- In a continuous gas phase, oil and water droplets settle, water droplets settle faster than oil droplets, so the oil droplet settling is controlling and is considered from the vessel top to the Normal Operating Level.
- In a continuous oil phase, the gas bubbles rise, and the water droplets settle. The gas bubbles rise faster so the water droplet settling is controlling and is considered from the Normal Operating Level to the Normal Interface Level.
- In a continuous water phase, the gas bubbles and the oil droplets rise. The gas bubble rise faster and so the oil droplet rising from the bottom of the vessel to the Normal Interface Level is controlling.

Eqs. (69) and (70) below are examples developed based on the separation of oil droplets from the gas continuous phase. The same procedure is used to determine the length required for gravity settling for the oil and water phases, respectively.

$$t_r = L_{gr}/U_g \tag{69}$$

$$U_g = Q_g/A_g \tag{70}$$

Retention time is set to be equal to the length of the gravity settling section divided by the flow velocity as in Eq. (69). The flow velocity can be calculated by dividing the flow rate by the area as in Eq. (70). Substituting Eq. and solving for Lgr gives Eq. (71) which is the length required for gravity settling of the droplets or bubbles out of a continuous phase.

$$t_r = L_{gr}A_g/Q_g \tag{71}$$

Time for oil droplets to settle through the gas phase in Eq. (68) can be expressed as;

$$t_{og} = \frac{(D_i - h_{NOL})}{U_{og}} \tag{72}$$

$$L_{gr1} = \frac{Q_g(D_i - h_{NOL})}{U_{og}(\text{VA} - A_{NOL})} \tag{73}$$

The settling velocity (in this case, of oil out of gas phase) is determined by equating the gravity force to the drag force. Calculating the settling velocity using Eqs. (74) and (75) requires an iterative process which starts with an assumption for the initial value of the drag coefficient. The terminal velocity is calculated and used to calculate the Reynolds number which in turn is used to calculate the drag coefficient. This value is then used as the input into the terminal velocity Equation and the

procedure is repeated until the difference between the calculated and the assumed values are equal.

$$u_{og} = \sqrt{\left[\frac{1.333 d_p g(\rho_o - \rho_g)}{C_D \rho_g}\right]} \quad (74)$$

$$N_{Re} = \frac{\rho U_{og} d_p}{\mu} \quad (75)$$

$$C_D = 0.34 + \frac{24}{N_{Re}} + \frac{3}{\sqrt{N_{Re}}} \quad (76)$$

The length required for settling water from the oil continuous phase and that of rising oil from water continuous phase are obtained using Eqs. (77) and (78);

$$L_{gr2} = \frac{Q_o(h_{NOL} - h_{NIL})}{U_{wo}(A_{NOL} - A_{NIL})} \quad (77)$$

$$L_{gr3} = \frac{Q_w h_{NIL}}{U_{ow} A_{NIL}} \quad (78)$$

3.1.2.3. Logical and geometric constraints. The third group of constraints was derived from the maximum dimensions allowed for road transport in the UK and the US. Most of the work carried out on the sizing of three-phase separators does not consider the transportation of these vessels from the manufacturing to the operation sites. Hence, it is necessary to ensure all manufactured vessels are within the road transport limits. From the literature, the maximum length that can be transported by road is 18.75m and a diameter of 4.23m.

Therefore, the following constraints were developed.

- The maximum separator diameter (VD) should not be more than 4.23m

$$VD = D_i + 2t_c \leq 4.23m \quad (79)$$

- The maximum separator length (LT) should not be more than 18.75m

$$\mathrm{LT} = \mathrm{VL} + 2(\mathrm{HL} + \mathrm{tc}) \leq 18.75m \quad (80)$$

$$\mathrm{HL} = \mathrm{Di}/4 \quad (81)$$

3.1.2.4. Decision variables constraints. The final group of constraints are set on the decision variables. For optimisation to proceed, it is necessary to set some inputs at the start and to constraint them towards a possible solution. Therefore, the set inputs i.e. internal diameter (Di), length of gravity settling section (Lgr), heights of normal operating, and normal interface levels (hNOL, hNIL) are constrained to be greater than 0.

$$D_i, L_g, h_{NLL}, h_{NIL} \geq 0 \quad (82)$$

Note that the constraints can be easily modified to fit the user's needs. For example, the constraints can be modified to include oversized loads, remove shut down or alarm levels if there is no requirement to shut down the process or if there will be no time for operators to react. Once the separator dimension, liquid levels, and capital (equipment) cost are obtained from the minimisation function, the separator fixed capital cost can then be determined.

3.2. Excel spreadsheet model design

The Capital cost model was formulated into an excel spreadsheet. User-defined functions (UDF) and subroutines were designed to gain accuracy and speed up the calculation process using Visual Basic Application (VBA). The model uses a Graphic user interface (GUI) also developed using VBA for simplicity and ease of usage.

The excel spreadsheet model comprises 4 tabs; the first tab contains the nomenclature which states the meaning of all the abbreviations used in the model. The user can select the button to insert all the fluid properties and operating conditions (see Figure 4). Default values are given for all inputs but can be overwritten if propriety data is available for all or some of the variables. A second option is provided for data relating to operating costs including the cost of crude oil, cost of Produced water treatment, cost of electricity, and transportation cost. Once submitted the data is automatically stored into the capital and operating cost models.

The capital cost tab uses the input variables supplied by the user to calculate the separator capital cost. The capital cost page is divided into four sections from left to right. The first section is where the input variables are stored. The second section consists of intermediate variables. These are calculated from the input variables. Three buttons that call the goal seek function were developed using VBA to solve the iterative process of calculating the terminal velocities of oil in gas, oil in water and water in oil. The third section is comprised of the fitted variables. These variables are initially calculated using initial guesses and later fitted by the GRG solver. The objective function and decision variables fall under this section. The last group of parameters are the constraints that were imposed on the objective function. The output from the two models in terms of separator diameter, length, and various liquid levels within the separator and capital cost are displayed in the output tab.

3.3. Numerical sizing example for capital cost model

To study the economics of the separation process, a numerical example is provided. It involves calculating the appropriate separator length, diameter, liquid levels, settling velocities, drag coefficients, outlet gas, oil and water diameters, equipment cost, and cost related to the day to day operation of the separator.

3.3.1. Numerical sizing example question

Design a horizontal three-phase separator with a flat plate inlet diverter and overflow weir to separate a mixture of gas, oil, and water and determine the total investment required to set up the equipment. The fluid properties and operating conditions are presented in Table 1. Other input variables and physical constants are given in Table 2.

3.3.2. Numerical sizing example results

The step by step procedure developed is presented in Appendix 1. This was used to obtain the results presented in Table 3. The GRG solver used a solution time of 0.093seconds and 7 iterations to obtain converged solution with the following values for the decision variables; Di = 1.48m, Le = 7.13m, hNOL = 0.74m, hNIL = 0.37m, L/D = 5.

Appendix 2 presents more information about the status and values of the constraints at optimal conditions. The status column indicates the constraints constraining the design i.e. in this case the three safety constraints with binding status. All other constraints are not binding which means there is some slack between the constraint and its limit. For example, if the gas, oil and water capacities are analysed, it will be observed that a slack of 0.04, 7.10 and 7.11 were obtained. What this means is that for this diameter, the length of the gravity settling section could be reduced to 7.11m which is the maximum value among the three values and the specified bubble/drop sizes would still have been separated.

4. Comparison with other models

An excel spreadsheet was built for [4, 14, 33, 34], and the current work. For the comparison, flow rates of 3100–8200 m^3/h (3 to 7MMSCFD), 20–46 m^3/h (3000–7000BPD), and 7–33 m^3/h (1000–5000BPD) were used for gas, oil, and water respectively.

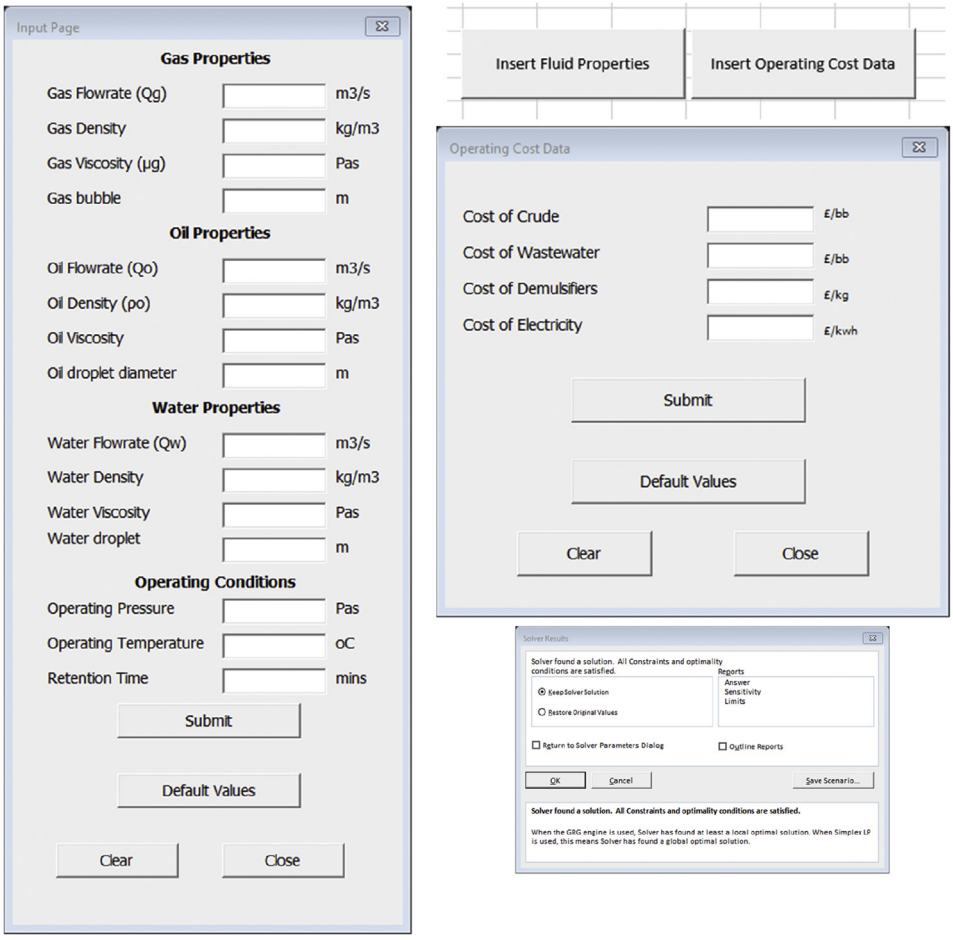

Figure 4. Screenshots of input page for developed model.

Table 1. Fluid properties for three-phase separator numerical sizing example.

Fluid Properties	Gas	Oil	Water
Flow rate (m^3/hr)	5400	100	5
Density (kg/m^3)	1.225	850	1000
Viscosity (kg/m-s)	1.7894e-05	0.046	0.001

Table 2. Input variables and physical constants.

Variable	Symbol	Value
Norsok Residence Time	Δt_{Nor}	30 Seconds
Norsok Residence Height	Δh_{Nor}	0.10m
Safety Height	Δh_s	0.175m
Density of Steel	ρ_s	7850 kg/m^3
Separator Inlet Length	L_i	0.10m
Cost Factor for Vessel Shell	F_c	5$/kg
Joint Efficiency	E	1
Corrosion Allowance	t_c	0.0032
Tensile Strength	σ	950×10^5
Length of Oil Weir	L_{weir}	0.01

These flow rates were based on real data (see Figure 5). The data shows that the initial production contains small amount of water with high gas and oil fractions. However, after some years, the oil and gas production declined while the water production increased significantly.

During oil and gas production, the gas phase is usually much higher than the liquid phase. In fact, the gas can be as high as 95% with the liquid (oil and water) taking up only about 5% of the total production volume fraction. As such the comparison carried out focused on similar

Table 3. Numerical sizing example results.

Variable	Symbol	Value
Separator Cost	C	£33,685
Separator Internal Diameter	Di	1.48m
Separator Length	VL	7.35m
High-High Liquid Level	h_{HHLL}	0.90m
High Liquid Level	h_{HLL}	0.82m
Normal Operating Level	h_{NOL}	0.74m
Low Liquid Level	h_{LLL}	0.66m
Low-Low Liquid Level	h_{LLLL}	0.58m
Weir Height	h_{Wr}	0.57m
High-High Interface Level	h_{HHIL}	0.53m
High Interface Level	h_{HIL}	0.45m
Normal Interface Level	h_{NIL}	0.37m
Low Interface Level	h_{LIL}	0.29m
Low-Low Interface Level	h_{LLIL}	0.21m
Diameter of Gas Outlet	dng	0.744m
Diameter of Oil Outlet	dno	0.14m
Diameter of water outlet	dnw	0.07m
Seam to Seam Length	LT	7.36m
Shell Thickness	tcs	0.01m
Separator Diameter	D	1.17m

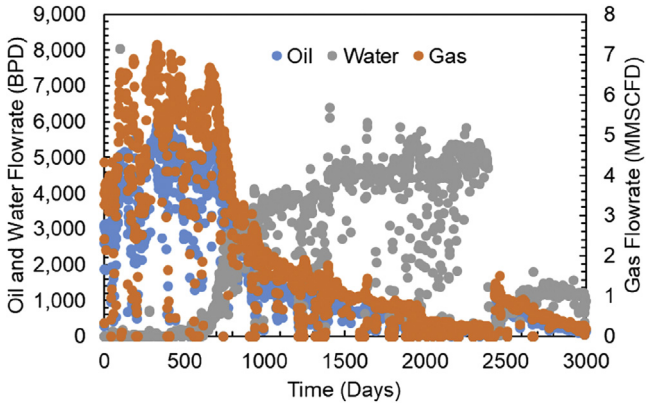

Figure 5. Daily gas, oil and water production data.

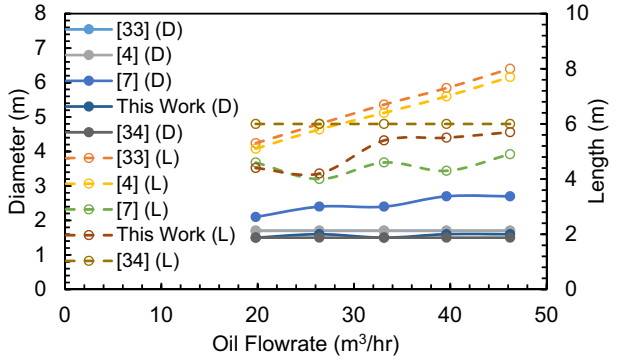

Figure 6. Length and diameter against Oil Flow rate at Fixed Gas and Water Flows. Where [33] is Abdel Aal, Aggour and Fahim (2003) [4], Arnold and Stewart (2008) [7], is Svrcek and Monnery (1994) and [34] is William (2015).

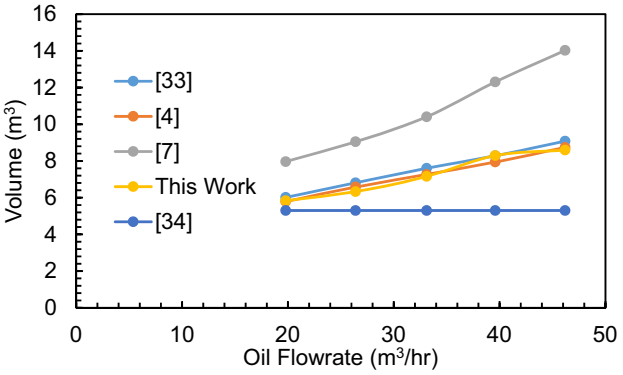

Figure 7. A graph of volume against Flowrate at Fixed Gas and Water Flows.

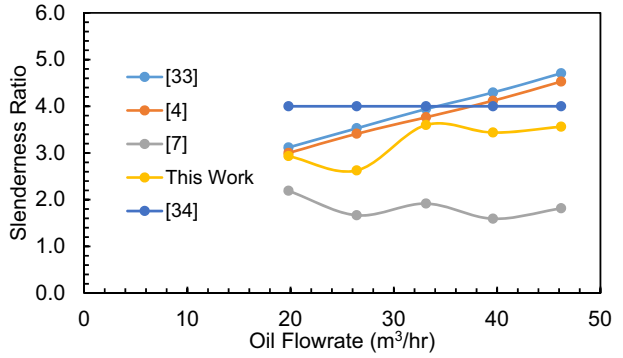

Figure 8. A graph of Slenderness ratio against Oil Flow rate at Fixed Gas and Water Flows.

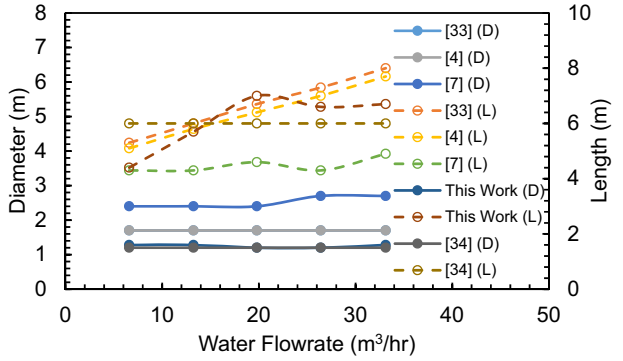

Figure 9. Diameter and Length against water flow rate at Fixed Gas and Oil Flows.

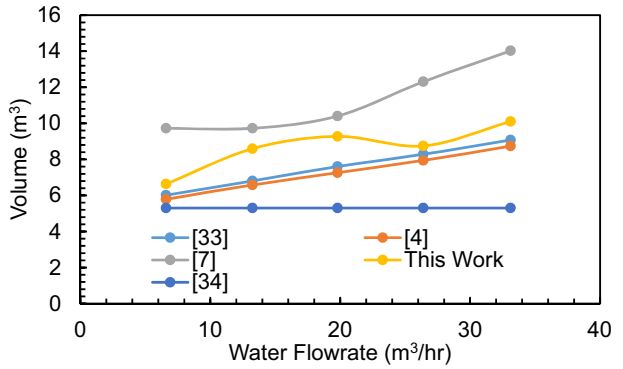

Figure 10. A graph of volume against Flowrate at Fixed Gas and Oil Flows.

flow conditions (i.e. high gas to liquid ratio). The effect of increasing the flow rate of each phase on the separator sizing models was determined and presented in the following subsections.

4.1. Comparison of models at fixed gas and water flow rates

Initially it was decided to fix the gas and water flow rates at 5886 m^3/h (5MMSCFD) and 33.12 m^3/h (5000BPD) respectively and vary the oil flow rate from 19.8 to 46.2 m^3/hr (3000–7000BPD) to investigate the effect of oil fraction on the separator size. Results from these comparisons are presented in Figure 6.

The William [34] model produces separator dimensions that do not change with increasing oil flow rate. This method is more closely constrained than the others given the slenderness ratio is fixed at four and the separator has to operate at 80% full of liquids. Taken together these constraints fix the separator dimensions for all oil flows.

The calculators of [33] and [4] produce very similar results. A linear relationship is seen between the increase in oil flow rate and the length of the vessel. This is not surprising because these models were developed to use droplet settling theory for gas-liquid separation and retention time theory for liquid-liquid separation. In both cases, it was found that liquid-capacity constrained the design. Given this, the diameter of the separator is fixed, and the length is set as being proportional to the volume derived as the product of flow rate and retention time.

Figure 7 presents the volume of the separator predicted by each of the models. The results show that an increase in the flowrate causes an increase in the volume of the separator for all models except [34]. The current model, and [7] were developed from the droplet settling theory for both gas-liquid separation and liquid-liquid separation. It would, therefore, be reasonable to see good agreement between these models. What is interesting however, is that the current model data gives a similar volume to the retention time-based methods, while the [7] predict a volume that is systematically larger than the other methods. Note that the current model seems to remove the discrepancy between the two theories with an absolute error of $\pm 0.35 m^3$.

Figure 8 presents a plot of slenderness ratio as a function of the oil flow rate. Again, the trend obtained from the current model more closely matches that obtained from the retention time models. The results of [7] are systematically low and show a slight decrease in the ratio as the flow is increased. The consequences of using the [7] are that the increase in diameter would produce a more expensive separator because of the increase in material thickness required to maintain the internal pressure.

Overall, it may be concluded that the use of optimisation of cost in the model leads to a design that is more in line with those predicted by retention theory without the need for experimentation.

4.2. Comparison of models at fixed gas and oil flow rates

The next step was to fix the gas and oil flow rates at 5886 m^3/h and 46.2 m^3/h respectively and vary the water flow rate from 6.6 to 33.12 m^3/hr to investigate the effect of water fraction on the separator size. These results are reported in Figures 9 and 10. [34] was again found to produce constant dimensions and will not be discussed further.

All the diameters were found to be within 1.5–1.7 m excluding [7] as shown in Figure 8. Again, the diameters predicted by [7] method are systematically higher than the other methods. The length of separators modelled using [4,33] increase linearly as the water flow rate increases. The current model produces separator length that also increases as the water flow rate increases.

Figure 10 presents the volume of the separators for fixed gas and oil flows. Similarly, an increase in the volume of the separators is obtained across all models except [34] as the water flowrate increase. [7] predicted a separator with the largest volume. [4,33] predicted a linear trend with increasing water flowrate. The current model predicted a volume less than [7] but greater than [4,33].

For the slenderness ratio, [7] trend is again systematically low and does not show a rise with increasing flow rate (see Figure 11). The lower slenderness ratios of less than 2 across the range predicted by [7] could be a cause for concern as low ratios lead to more expensive designs. Finally, it is again concluded that the current model results show similar trends to the retention time methods.

4.3. Comparison of models at fixed oil and water flow rates

Finally, it was decided to keep the oil and water flow rates constant and vary the gas flow to check its effects on the separator sizes for different separator sizing models. Initially the gas flow was varied from 3000 to 8400 m^3/hr and the results are presented in Figures 12 and 13. Fixed dimensions were obtained for all the models. This indicated that liquid capacity is constraining the design in all the models.

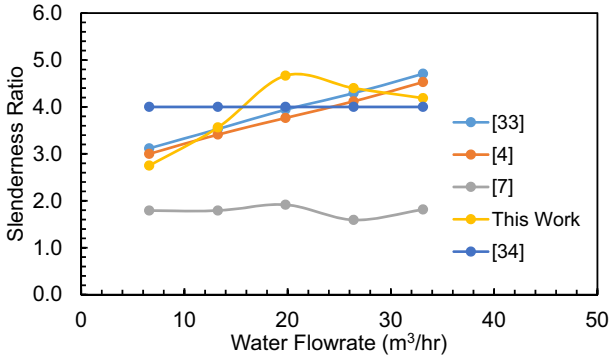

Figure 11. Slenderness ratio against Water Flow rate at Fixed Gas and Oil Flows.

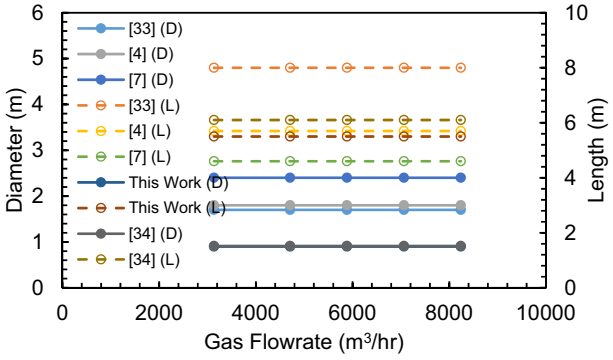

Figure 12. Diameter and Length against Gas Flow rate at Fixed Oil and Water Flows.

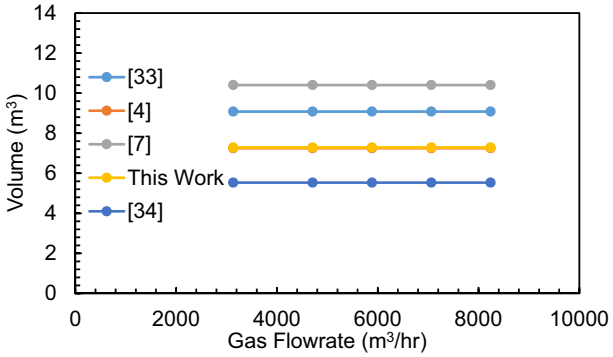

Figure 13. A graph of volume against Flowrate at Fixed Oil and Water Flows.

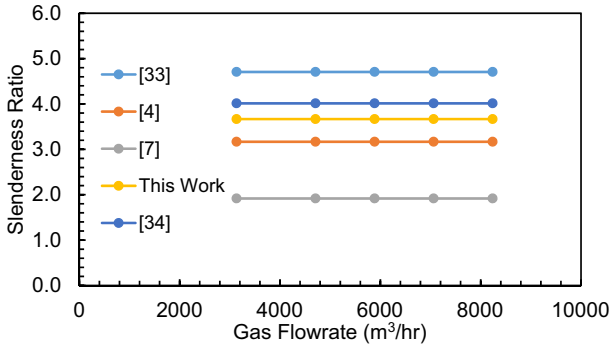

Figure 14. Slenderness Ratio against Gas Flow rate at Fixed Oil and Water Flows.

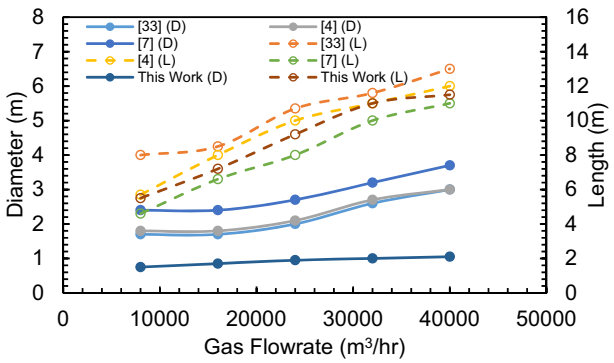

Figure 15. Diameter and Length against flowrates for high gas flowrates.

Figure 13 presents the volume predicted by the chosen models for fixed oil and water flows. As seen in Figure 12, fixed dimensions were obtained for the set of gas flows used for this comparison. Therefore, fixed separator volumes were obtained. The results also showed that the current model closely matches the volume predicted by Arnold and Stewart (2008).

The slenderness ratio was found to be between 2 to 5 as shown in Figure 14. [33] predicted a slenderness ratio of 4.7, [34] 4, the current model 3.7. [4] 3.2 and [7] 2.

The gas flowrates were further increased from 5000 to 25000 (m^3/hr) with increments of 5000 to try to find the point at which gas flow becomes significant. Figure 15 presents the results for the higher gas flows. For this comparison, [34] was not included because it was developed for low gas-oil ratio. A similar trend was obtained for [4,33], and the current model for both diameters and lengths of the separators which increase as the gas flowrate increases. [7] model predicted higher dimensions for both the separator length and diameter. This is then followed by [4,33] which as seen in previous comparisons predicted very similar results. Finally, the current model predicted the least separator length and diameter for the chosen flowrates.

Figure 16 presents the volume of the liquid collection section of the separator. All models predict results within 20% difference for gas flowrates of 8000 to 2400 m^3/h. A further increase in the gas flow results in the current model predicting the least volume. [4,33] again predicted similar results, while [7] predicted the largest volume.

Figure 17 presents the slenderness ratios for the models at very high gas flows. A similar trend with a range of 3–5 was observed in the two models developed based on retention time theory. The current model predicted a slenderness ratio of 3.5–5.2 which is the highest. Finally, [7] predicted the least slenderness ratio of 2.5.

Overall, it may be concluded that the use of capital cost optimisation in the current model leads to a design that is more in line with those predicted by retention theory without the need for experimentation.

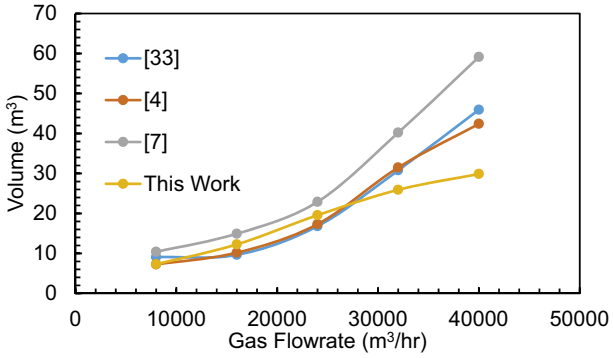

Figure 16. A graph of volume against Flowrate at Fixed Gas and Oil Flows.

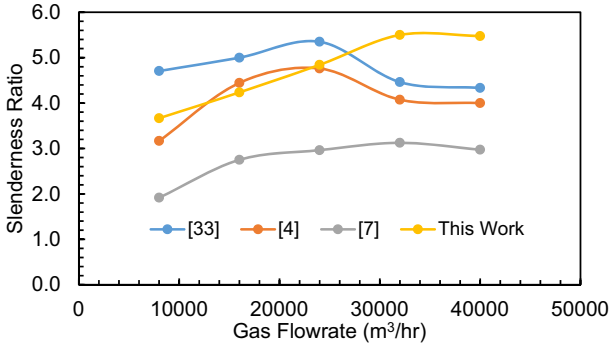

Figure 17. Slenderness ratio for very high gas flows.

5. Conclusion

The development of the optimisation model that aims to link the separator design with the cost associated with its construction has been presented. The paper covers the model development using GRG non-linear optimisation technique to minimise the capital cost of a horizontal three-phase separator. The objective function comprising of input, fitted and calculated variables was minimised subject to some constraints. The constraints were grouped into four.

- The first group of constraints were set to ensure the various phases leave the separator through their designated outlets.
- The length of the gravity settling section was set as the second group of constraints.
- Logical and geometrical constraints were also set to ensure ease of transportation from the manufacturing to the operation sites.
- The decision variables were constrained towards a possible solution.

The developed model was built into an excel spreadsheet in conjunction with Excel VBA and Add-in solver and compared with 4 other extant models. Based on the comparison conducted in this work, the following conclusions can be made.

1. The models proposed by [4] and [33] are based on the assumption that the separator operates half full. The models predicted results that are directly proportional to the retention time and liquid flow rate. Equal changes in lengths are observed for every change in the liquid flow rate. No change was found when the gas flow rate increases for the chosen flow rates. The model does not give adequate information about the separator.
2. [4] is also based on the assumption of half-filled separators. Separators sized using this model will tend to be more costly due to its wider diameters obtained in all the three sets of comparisons conducted.

The model is also based on several tables look-ups and manual iterations which makes it less accurate.

3. For all the cases investigated, a linear trend was obtained for [34]. This is attributed to the constraints in the model.
4. Finally, the model developed in this paper gives more details such as the nozzle sizes, liquid levels, settling velocities of Oil and Water, weir height, and vessel wall thickness. The model predicted separator sizes similar to retention time models without the need for experimentation.

Declarations

Author contribution statement

Tariq Ahmed: Conceived and designed the experiments; Performed the experiments; Analyzed and interpreted the data; Wrote the paper.

Paul, A. Russell: Conceived and designed the experiments; Analyzed and interpreted the data; Contributed reagents, materials, analysis tools or data; Wrote the paper.

Nura Makwashi, Faik Hamad & Samantha Gooneratne: Analyzed and interpreted the data; Wrote the paper.

Funding statement

This work was supported by Petroleum Technology development Fund (PTDF) Nigeria.

Competing interest statement

The authors declare no conflict of interest.

Additional information

Supplementary content related to this article has been published online at https://doi.org/10.1016/j.heliyon.2020.e04065.

References

[1] IEA., World Energy Outlook 2017, Organisation for Economic Co-operation and Development, OECD, 2017.
[2] M. Vileiniskis, R. Remenyte-Prescott, D. Rama, J. Andrews, Fault detection and diagnostics of a three-phase separator, J. Loss Prev. Process. Ind. 41 (2016) 215–230.
[3] J.H. Song, B.E. Jeong, H.J. Kim, S.S. Gil, Three-phases separator sizing using drop size distribution, in: Offshore Technology Conference, 2010.
[4] K. Arnold, M. Stewart, in: " K. Arnold, M. Stewart (Eds.), Chapter 5 - Three-phase Oil and Water Separation, Gulf Professional Publishing, Burlington, 2008, pp. 244–315.
[5] A. Ghaffarkhah, M.A. Shahrabi, M.K. Moraveji, 3D computational-fluid-dynamics modeling of horizontal three-phase separators: an approach for estimating the optimal dimensions, SPE Prod. Oper. 33 (04) (2018) 879–895.
[6] K.E. Arnold, P.J. Koszela, Droplet Settling vs. Retention Time Theories for Sizing Oil/Water Separator, 1987.
[7] W.D. Monnery, W.Y. Svrcek, Successfully specify three-phase separators, Chem. Eng. Prog. 90 (29) (1994).
[8] M.L. Powers, Analysis of gravity separation in freewater knockouts, SPE Prod. Eng. 5 (01) (1990) 52–58.
[9] T. Ahmed, F. Hamad, P.A. Russell, The Use of CFD Simulations to Compare and Evaluate Different Sizing Algorithms for Three-phase Separators, 2017.
[10] T. Ahmed, P.A. Russell, F. Hamad, S. Gooneratne, Experimental analysis and computational fluid dynamics modelling of pilot-scale three-phase separators, SPE Prod. Oper. (2019).
[11] N. Kharoua, L. Khezzar, H. Saadawi, CFD modelling of a horizontal three-phase separator: a population balance approach, Am. J. Fluid Dynam. 3 (4) (2013) 101–118.
[12] A.P. Laleh, W.Y. Svrcek, W. Monnery, Computational fluid dynamics-based study of an oilfield separator–Part II: an optimum design, Oil Gas Facil. 2 (01) (2013) 52–59.
[13] T. Frankiewicz, C.-M. Lee, Using Computational Fluid Dynamics (CFD) Simulation to Model Fluid Motion in Process Vessels on Fixed and Floating Platforms, 2002.
[14] N. Kharoua, L. Khezzar, H.N.H. Saadawi, Using CFD to model the performance of retrofit production separators in abu Dhabi, in: Abu Dhabi International Petroleum Conference and Exhibition, 2012.
[15] Y. Lu, J.M. Lee, D. Phelps, R. Chase, Effect of internal baffles on volumetric utilization of an FWKO–A CFD evaluation, in: SPE Annual Technical Conference and Exhibition, 6, 2007.
[16] E.O. Grodal, M.J. Realff, Optimal design of two-and three-phase separators: a mathematical programming formulation, in: SPE Annual Technical Conference and Exhibition, 1999.
[17] M. Mostafaiyan, M.R. Saeb, A.E. Alorizi, M. Farahani, Application of evolutionary computational approach in design of horizontal three-phase gravity separators, J. Petrol. Sci. Eng. 119 (2014) 28–35.
[18] H. Silla, Chemical Process Engineering: Design and Economics, United States of America: CRC Press, 2003.
[19] R. Smith, Chemical Process: Design and Integration, John Wiley & Sons, 2005.
[20] W.D. Seider, J.D. Seader, D.R. Lewin, S. Widagdo, Product and process design principles: synthesis, Anal. Eval. York Wiley (2004).
[21] M. Ray, M. Sneesby, Chemical Engineering Desing Project, 1989.
[22] H.J. Lang, Simplified approach to preliminary cost estimates, Chem. Eng. 55 (6) (1948) 112–113.
[23] S. Lemmens, Cost engineering techniques and their applicability for cost estimation of organic Rankine cycle systems, Energies 9 (7) (2016) 485.
[24] K. Arnold, M. Stewart, in: K. Arnold, M. Stewart (Eds.), Chapter 4 - Two-phase Oil and Gas Separation, Gulf Professional Publishing, Burlington, 2008, pp. 150–243.
[25] G.D. Ulrich, A Guide to Chemical Engineering Process Design and Economics, Wiley, New York, 1984.
[26] W.L. Winston, Operations Research Applications and Algorithms, *Inc.*, Belmont, CA, 1994.
[27] C.-M. Lee, E. van Dijk, M. Legg, J. Byeseda, Field confirmation of CFD design for FPSO-mounted separator, in: Offshore Technology Conference, 2004.
[28] A. Boiler, P.V. Code, Section VIII Division 1, *UG-126 Press*. Reli. Valves to UG-129 Marking, ASME Int., New York, 2010.
[29] L.E. Brownell, E.H. Young, Process Equipment Design: Vessel Design, John Wiley & Sons, 1959.
[30] S. Rahimi, Three Phase Separators Inlet Devices, 2013. http://chemwork.org/PDF/board/Three%20phase%20Separator%20-%20Inlet%20Devices.pdf.
[31] R. Chin, The savvy separator series: Part 2 the effect of inlet geometries on flow distribution, Oil Gas Facil. 4 (04) (2015) 26–31.
[32] P. Design, Norsok standard–P100, Nor. Pet. Ind. 9–22 (2006).
[33] H.K. Abdel-Aal, M.A. Aggour, M.A. Fahim, Petroleum and Gas Field Processing, CRC Press, 2015.
[34] W.P. Dokianos, A simplified approach to sizing 2 and 3 phase separators for low GOR and low pressure onshore production batteries, in: SPE Production And Operations Symposium, 2015.